J. Fluid Mech. (1981), *vol.* 103, *pp.* 241–255
Printed in Great Britain

Effects of truncation in modal representations of thermal convection

By PHILIP S. MARCUS†
Center for Radiophysics and Space Research, Cornell University

(Received 8 November 1979 and in revised form 7 May 1980)

We examine the Galerkin (including single-mode and Lorenz-type) equations for convection in a sphere to determine which physical processes are neglected when the equations of motion are truncated too severely. We test our conclusions by calculating solutions to the equations of motion for different values of the Rayleigh number and for different values of the limit of the horizontal spatial resolution. We show how the gross features of the flow such as the mean temperature gradient, central temperature, boundary-layer thickness, kinetic energy and temperature variance spectra, and energy production rates are affected by truncation in the horizontal direction. We find that the transitions from steady-state to periodic, and then to aperiodic convection depend not only on Rayleigh number but also very strongly on the horizontal resolution of the calculation. All of our models are well resolved in the vertical direction, so the transitions do not appear to be due to poorly resolved boundary layers. One of the effects of truncation is to enhance the high-wavenumber end of the kinetic energy and thermal variance spectra. Our numerical examples indicate that, as long as the kinetic energy spectrum decreases with wavenumber, a truncation gives a qualitatively correct solution.

1. Introduction

Recently, there has been much interest in computing solutions to the nonlinear equations that govern thermal convection by using a Galerkin method in which the velocity and temperature fields are represented by a finite number of modes. In applying these truncated models to a convecting fluid in which the Rayleigh number is large, such as the convection zone of a star (Marcus 1980*a*, *b*; Latour *et al.* 1976; Toomre *et al.* 1976) we should be somewhat cautious in taking too literally the exact pattern of the calculated velocity and temperature fields. However, the gross features of the computed flow such as the Nusselt number, kinetic energy spectrum, thermal variance spectrum, mean temperature gradient, central temperature, and size of the boundary layers may indeed be quite accurate and it is worth-while to determine how sensitive these quantities are to the truncation.

In laboratory flows at more moderate Rayleigh numbers there have been recent measurements of the bifurcations as the Rayleigh number is increased. Gollub & Benson (1980) have carefully measured, as a function of Rayleigh number, the transitions from steady state to periodic, to one or more states of period doubling, quasi-periodicity or phase locking and then finally to non-periodicity. In trying to explain

† Present address: Department of Mathematics, Massachusetts Institute of Technology, Cambridge, Mass.

0022–1120/81/4637–3100 $02.00

these bifurcations theorists have performed modal calculations. Unfortunately, the number of bifurcations and types of bifurcations produced in the calculations strongly depend on how many modes are retained in the truncation. For example, in a fluid with Prandtl number of 10, Lorenz (1963) has found there is one inverted bifurcation that takes the flow from a steady state to a strange attractor; whereas Curry (1978) for the same Prandtl number found that with a more extensive 14-component model the flow exhibits a normal bifurcation to periodic motion, followed by a bifurcation to period doubling. The flow then bifurcates to an attracting torus and finally changes to non-periodic motion. Toomre, Gough & Spiegel (1977), and Marcus (1978) found the surprising result that if the vertical structure is finely resolved but only one Fourier mode is retained in the horizontal (single-mode theory) then there are no bifurcations. The fluid remains in a stable, steady-state regardless of Rayleigh number. For a Prandtl number of unity and a 39-mode truncation McLaughlin & Martin (1975) found four bifurcations in a fluid that initially was in a steady state with rolls aligned along the y axis: the first transition to periodic flow, the second to weakly non-periodic motion, the third to a periodic state and the last to non-periodic motion. When they reduced the number of modes in their calculation so that there were only three different wavelengths in the y direction, they found that there was no final transition to non-periodicity. These modal conclusions all support Ruelle & Takens' (1971) assertion that after at most 4 normal bifurcations the solutions must be non-periodic in time. However, it is important to know whether the bifurcations predicted by the modal equations are inherent to the full nonlinear equations that govern the convective motion or are a general property of the nonlinear, coupled, autonomous equations that govern the finite modes of the truncation. If the truncated equations of motion do not have sufficient spatial resolution to model the physically important processes that occur in a convecting fluid, then the bifurcations of the truncated equations may not be related in any qualitative way to the actual transitions observed in the laboratory.

The purpose of this paper is to examine the solutions to truncated modal equations for convection in a sphere and to determine which qualitative features of the solutions represent real physical processes in the fluid and which features are due solely to the effects of truncation. In § 2 of this paper we briefly review the Galerkin multi-mode equations (including single-mode and Lorenz) for spherical convection. We attempt to describe the physics that each system of equations models, which physical processes are neglected by the various truncation schemes, and what artificial constraints each model imposes on its solutions.

For multi-mode calculations that include more than one horizontal wavelength, we find that as the Rayleigh numbers increase the solutions pass from a steady state to one or more states periodic in time. As the Rayleigh number increases further the solutions eventually become aperiodic. For a Rayleigh number of 10^5, our truncation with 168 modes produces a steady state. We find (holding the Rayleigh number and the resolution in the radial direction fixed) that, as we decrease the number of horizontal modes in the Galerkin expansion, there is a transition from steady-state convection to a solution that is periodic in time. As the number of modes is decreased still further, the solutions become aperiodic. In § 3 we describe these solutions as well as those for a Rayleigh number of 10^4 where the convection is time independent for all truncations. By computing how the energy spectra, convective flux, and temperature gradient

change as a function of the severity of truncation for both Rayleigh numbers, we not only show how the gross features of the flow are affected by the truncation, but also provide a possible explanation for the time dependence of our solutions. Our conclusions appear in § 4.

2. Approximations needed for the Lorenz, single-mode and multi-mode models

Convection in a Boussinesq fluid is governed by the Navier–Stokes continuity and thermal-diffusion equations, and the Boussinesq equation of state (see, for example, Chandrasekhar 1961). A standard technique used to simplify these coupled, nonlinear partial differential equations is the Galerkin method. The thermodynamic quantities and velocity are expanded as an infinite sum of coefficients multiplied by orthonormal functions and substituted into the governing equations. Then, depending on how many of the coefficients are solved and how many are arbitrarily set equal to zero, one arrives at a Lorenz, single-mode, or multi-mode model.

(*a*) *Review of the multi-mode equations*

Let us consider convection in a self-gravitating sphere of Boussinesq fluid with thermal expansion coefficient α, heat capacity C_p, kinematic viscosity ν, thermal diffusivity k, radius d, and a heat source $H(r)$ in the fluid. Each scalar quantity, such as the temperature, is written as a sum of its mean, $\langle T(r,t)\rangle$, and fluctuating, $\tilde{T}(r,\theta,\phi,t)$, parts, where

$$\langle T(r,t)\rangle = \int_{4\pi} T(r,\theta,\phi,t)\, d\Omega/4\pi \tag{2.1}$$

and

$$\tilde{T}(r,\theta,\phi,t) = 2(2\pi)^{\frac{1}{2}} \sum_{l=1}^{\infty} \Bigg\{ \sum_{m=1}^{l} [T_{\mathrm{Re},l,m}(r,t)\,\mathrm{Re}\,(Y^{l,m}) + T_{\mathrm{Im},l,m}(r,t)\,\mathrm{Im}\,(Y^{l,m})] + 2^{-\frac{1}{2}} T_{\mathrm{Re},l,0}(r,t)\, Y^{l,0} \Bigg\}. \tag{2.2}$$

$\mathrm{Re}\,(Y^{l,m})$ and $\mathrm{Im}\,(Y^{l,m})$ are the real and imaginary parts of the spherical harmonic. The velocity is written as a sum of its poloidal $\mathbf{v}_p$ and toroidal $\mathbf{v}_T$ parts which are derived from scalar fields ω and ψ;

$$\mathbf{v}_p = \nabla[\partial(r\omega)/\partial r] - (r\nabla^2\omega)\,\hat{e}_r, \tag{2.3}$$

$$\mathbf{v}_T = r\nabla \times (\psi \hat{e}_r). \tag{2.4}$$

Substituting expressions (2.3) and (2.4) into the equations of motion yields the equations for the coefficients for the temperature T, pressure P, gravitational potential Φ, and velocity $\mathbf{v}$ (Marcus 1980*a*):

$$\partial\omega_{\gamma,l,m}/\partial t = -r[l(l+1)^{-1}[Rs\,\sigma\, rT_{\gamma,l,m} + \partial(P_{\gamma,l,m} + \Phi_{\gamma,l,m})/\partial r] + \sigma\,\mathscr{D}_l(\omega_{\gamma,l,m}) - l(l+1)^{-1}\{r\hat{\mathbf{e}}_r \cdot [(\mathbf{v}\cdot\nabla)\,\mathbf{v}]\}_{\gamma,l,m}, \tag{2.5}$$

$$\partial\psi_{\gamma,l,m}/\partial t = \sigma\,\mathscr{D}_l(\psi_{\gamma,l,m}) - l(l+1)^{-1}\{r\hat{\mathbf{e}}_r \cdot \nabla \times [(\mathbf{v}\cdot\nabla)\,\mathbf{v}]\}_{\gamma,l,m}, \tag{2.6}$$

$$\partial T_{\gamma,l,m}/\partial t = \mathscr{D}_l(T_{\gamma,l,m}) - l(l+1)\,(\partial\langle T\rangle/\partial r)\,\omega_{\gamma,l,m}/r - [\mathbf{v}\cdot\nabla T]_{\gamma,l,m}, \tag{2.7}$$

$$\mathscr{D}_l(P_{\gamma,l,m}) = \sigma Rs\,(6T_{\gamma,l,m} + r\,\partial T_{\gamma,l,m}/\partial r) - r^{-2}\,\partial\{r[r\hat{\mathbf{e}}_r\cdot(\mathbf{v}\cdot\nabla)\,\mathbf{v}]_{\gamma,l,m}\}/\partial r - \{\nabla\cdot[(\mathbf{v}\cdot\nabla)\,\mathbf{v}]\}_{\gamma,l,m}, \tag{2.8}$$

$$\mathscr{D}_l(\Phi_{\gamma,l,m}) = -3\,\sigma Rs\,T_{\gamma,l,m}, \tag{2.9}$$

$$\langle\omega\rangle = \langle\psi\rangle = 0, \tag{2.10}$$

$$\frac{\partial\langle T\rangle}{\partial t} = r^{-2}\{\partial(r^2\,\partial\langle T\rangle/\partial r)/\partial r + \partial\mathscr{L}/\partial r - \partial\sum_{\gamma,l,m} rl(l+1)\,T_{\gamma,l,m}\omega_{\gamma,l,m}]/\partial r\}, \tag{2.11}$$

where $\mathscr{D}_l$ is the differential operator defined by its action on the scalar, f,

$$\mathscr{D}_l(f) \equiv [\partial^2(rf)/\partial r^2 - l(l+1)f/r]/r, \tag{2.12}$$

and where $\mathscr{L}(r)$ is the luminosity

$$\mathscr{L}(r) = 4\pi\int_0^r \langle H\rangle\, r'^2 dr'. \tag{2.13}$$

In equations (2.5)–(2.11), $Rs \equiv \alpha G d^3\mathscr{L}(d)/3k^2\nu C_p$ is the Rayleigh number, $\sigma \equiv \nu/k$ is the Prandtl number and γ stands for either Re or Im.

In equations (2.5)–(2.13) the unit of time is k/d^2, length is d, mass is ρd^3 and temperature is $\mathscr{L}(d)/4\pi\rho C_p dk$. Equations (2.5)–(2.10) may be thought of as the governing equations for each eddy or mode (γ, l, m) that makes up the total velocity field. The nonlinear terms in equations (2.5)–(2.13) such as $\{r\hat{\mathbf{e}}_r\cdot[\mathbf{v}\cdot\nabla)\,\mathbf{v}]\}_{\gamma,l,m}$ are the eddy–eddy interaction terms, with contributions from all other pairs of modes (γ', l', m') and (γ'', l'', m'') that obey certain selection rules. The selection rules and the explicit expressions for the nonlinear interactions are given in a previous paper (Marcus 1979) in terms of Wigner-3j symbols. For a sphere with an impermeable, stress-free boundary the velocity is constrained at $r = 1$ so that

$$\omega_{\gamma,l,m}(1) = 0, \tag{2.14}$$

$$\partial^2\omega_{\gamma,l,m}/\partial r^2|_{r=1} = 0, \tag{2.15}$$

$$\partial(\psi_{\gamma,l,m}/r)/\partial r|_{r=1} = 0. \tag{2.16}$$

We also require that the surface be isothermal:

$$T_{\gamma,l,m}(1) = 0. \tag{2.17}$$

We are free to choose the mean temperature to be zero at $r = 1$:

$$\langle T(r=1)\rangle = 0. \tag{2.18}$$

However, the gradient of the mean temperature (and therefore the flux) at $r = 1$ is free to vary. The central temperature, $\langle T(0)\rangle$, is also free to vary and is a measure of the efficiency of the overall convective flux. The lower the value of $\langle T(0)\rangle$, the more isothermal the fluid is. The central temperature is given by

$$\langle T(0)\rangle = -\int_0^1 \mathscr{L}r^{-2}\,dr - \int_0^1 \sum_{\gamma,l,m} l(l+1)\,T_{\gamma,l,m}\omega_{\gamma,l,m}r^{-1}\,dr - \frac{\partial}{\partial t}\int_0^1\left[\int_0^r r'^2\langle T(r')\rangle\,dr'\right]r^{-2}\,dr. \tag{2.19}$$

We must use the central temperature as a measure of the efficiency convection because the Nusselt number is not well defined for our boundary conditions.

(*b*) *Sufficient conditions for a good truncation*

The infinite set modal equations (2.5)–(2.13) for the coefficients can only be solved by arbitrarily setting some of the coefficients equal to zero (or some other functional form) and explicitly solving for the remaining finite set of coefficients. What are the consequences of setting some modes equal to zero? The equation for mean value of the temperature (2.11), is well approximated if and only if the term $\Sigma l(l+1)\omega_{\gamma,l,m}T_{\gamma,l,m}/r$, when summed over the finite set of kept modes, is nearly equal to what it would be if it were summed over all modes. Now, $\Sigma l(l+1)\,\omega_{\gamma,l,m}T_{\gamma,l,m}/r$ is equal to the convective flux and the contribution from each mode is just the convective flux carried by that particular eddy. Therefore equation (2.11) is well approximated if we keep those eddies that carry most of the flux in the Galerkin expansion. Similarly it can be shown that equations (2.5)–(2.8) are well approximated only if we include the modes that are responsible for (1) the production of kinetic energy from buoyancy forces, (2) the production of the temperature variance, $\frac{1}{2}\tilde{T}^2$, (3) the viscous dissipation of kinetic energy, (4) the dissipation of the temperature variance, and (5) those modes that provide the nonlinear cascade of energy from the production modes to the dissipative modes. We expect that the modes most responsible for production of the kinetic energy temperature variance and convective flux are the largest spatial modes. We also expect that if we wish to include all of the modes that are important in the cascade and dissipation of kinetic energy and temperature variance, we will have to retain all modes with Reynolds or Péclet numbers greater than 1.

(*c*) *The effects of truncations on the kinetic energy*

The rate at which kinetic energy $\partial(\int\frac{1}{2}v^2d^3r)/\partial t$ enters the fluids due to buoyancy is (Marcus 1980*a*)

$$E_{1n} = 4\pi\sigma Rs\int_0^1 \sum_{\gamma,l,m} l(l+1)\,T^{\gamma}{}_{,l,m}\omega_{\gamma,l,m}r^2\,dr. \tag{2.20}$$

There are no cross-terms between different modes on the right-hand side of equation (2.20) and each term represents the kinetic energy contribution from one mode (γ, l, m). However, combining equation (2.11) with (2.20) shows us that we can write E_{1n} in terms of the luminosity and temperature gradient:

$$E_{1n} = 4\pi\sigma Rs\int_0^1\left[\frac{\partial\langle T\rangle}{\partial r}r^3 + r\mathscr{L} - \frac{\partial}{\partial t}r\int_0^r r'^2\langle T(r')\rangle\,dr'\right]dr. \tag{2.21}$$

By numerical experimentation we have found that, no matter how few modes are kept in the Galerkin expansion, the mean temperature gradient becomes nearly isothermal in the sense that

$$\left|\frac{\partial\langle T\rangle}{\partial r}\right| \ll \frac{\mathscr{L}(r)}{r^2}. \tag{2.22}$$

Using equation (2.22) and taking the time average (denoted by double angle brackets) of equation (2.21), we obtain

$$\langle\langle E_{1n}\rangle\rangle \approx 4\pi\sigma Rs\int_0^1 \mathscr{L}(r)\,r\,dr. \tag{2.23}$$

We find that even the most severe truncations produce a close approximation to the correct value of $\langle\langle E_{1n}\rangle\rangle$.

The time-averaged value of the rate at which kinetic energy is dissipated, $\langle\langle E_{\rm out}\rangle\rangle$, must be equal to $\langle\langle E_{\rm in}\rangle\rangle$. $E_{\rm out}$ is given by

$$E_{\rm out} = -4\pi\sigma\int_0^1 \Big[r^{-1}\,\partial^2(rE)/\partial r^2 + \sum_{r,l,m}\{-[l(l+1)]^2 r^{-2}\omega_{\gamma,l,m}\mathscr{D}_l(\omega_{\gamma,l,m}) - l(l+1)\,r^{-2}\,(\partial(r\omega_{\gamma,l,m})/\partial r)\,\partial[r\mathscr{D}_l(\omega_{\gamma,l,m})]/\partial r - (l(l+1)\,\psi_{\gamma,l,m}\mathscr{D}_l(\psi_{\gamma,l,m})\}\Big] r^2\,dr, \tag{2.24}$$

where $E(r)$ is the kinetic energy of the fluid at radius r and is

$$E(r) = \frac{1}{2}\sum_{\gamma,l,m} l(l+1)\,[\{\omega^2_{\gamma,l,m}\,l(l+1) + [\partial(r\omega_{\gamma,l,m})/\partial r]^2\}/r^2 + \psi^2_{\gamma,l,m}]. \tag{2.25}$$

Again, there are no cross-terms between modes on the right-hand side of equation (2.24) and each term in the sum represents the dissipation due to one mode. If the high-wavenumber modes responsible for the viscous dissipation are not included in the Galerkin expansion (or if the modes that are responsible for the cascade of kinetic energy to the dissipative modes are not included) $\langle\langle E_{\rm in}\rangle\rangle$ will not be strongly affected. However, to keep $\langle\langle E_{\rm out}\rangle\rangle$ equal to $\langle\langle E_{\rm in}\rangle\rangle$ the fluid must compensate by dissipating more kinetic energy in the large-scale modes. From equation (2.24) we see that one way in which the rate of dissipation can be increased is by increasing the kinetic energy of the modes. We therefore expect the kinetic energy of a severely truncated system to be abnormally high. This increase will be evident in the numerical examples in the next section.

(d) The effect of truncation on the fluctuating thermal energy

The rate at which temperature variance is created in the fluid is

$$Q_{\rm in} = -4\pi\int_0^1 \frac{\partial\langle T\rangle}{\partial r}\, r \sum_{\gamma,l,m} T_{\gamma,l,m}\omega_{\gamma,l,m}\; l(l+1)\,dr. \tag{2.27}$$

Each term in equation (2.27) corresponds to the thermal input of one mode. Even though $|\partial\langle T\rangle/\partial r|$ will generally be much less than $\mathscr{L}/r^2$, we have found that, for fixed Prandtl and Rayleigh numbers, $|\partial\langle T\rangle/\partial r|$ can vary by an order of magnitude depending upon the number of modes kept in the Galerkin expansion. Therefore, $\langle\langle Q_{\rm in}\rangle\rangle$ (unlike $\langle\langle E_{\rm in}\rangle\rangle$) is a sensitive function of the truncation. The rate at which the temperature variance is dissipated is

$$Q_{\rm out} = -4\pi\sum_{\gamma,l,m}[(\partial T_{\gamma,l,m}/\partial r)^2 + l(l+1)\,r^{-2}T^2_{\gamma,l,m}]\,r^2\,dr. \tag{2.28}$$

If the Galerkin truncation does not include the thermally dissipative modes, the truncated solution will have to adjust itself so that $\langle\langle Q_{\rm out}\rangle\rangle$ is kept equal to $\langle\langle Q_{\rm in}\rangle\rangle$. The solution can increase the rate of thermal dissipation in the retained modes by increasing the thermal variance of the modes. However, unlike $\langle\langle E_{\rm in}\rangle\rangle$, $\langle\langle Q_{\rm in}\rangle\rangle$ is not constrained and the fluid can adjust to its inability to dissipate the thermal variance by decreasing $\langle\langle Q_{\rm in}\rangle\rangle$. Since $\langle\langle Q_{\rm in}\rangle\rangle$ is proportional to the mean-temperature gradient (equation (2.27)), the fluid can reduce its rate of production of thermal variance by becoming more nearly isothermal. In the next section we show numerical examples in which a truncated solution both increases $\langle\langle Q_{\rm out}\rangle\rangle$ by increasing its thermal variance and decreases $\langle\langle Q_{\rm in}\rangle\rangle$ by becoming more nearly isothermal.

(e) *Single-mode theory*

The severest truncation of a multi-mode expansion is to retain only one horizontal mode. This requires that the solution be of the form:

$$T(r,\theta,\phi,t) = \langle T(r,t)\rangle + \tilde{T}(r,t)\,h(\theta,\phi), \tag{2.29}$$

$$P(r,\theta,\phi,t) = \langle P(r,t)\rangle + \tilde{P}(r,t)\,h(\theta,\phi), \tag{2.30}$$

$$\omega(r,\theta,t) = \tilde{\omega}(r,t)\,h(\theta,\phi), \tag{2.31}$$

$$\psi = 0, \tag{2.32}$$

where $h(\theta,\phi)$ is an eigenfunction of the horizontal Laplacian, $(\nabla^2 - 1/r(\partial^2/\partial r^2)\,r)$. Because the toroidal modes are not involved in the convective flux, kinetic-energy production, or temperature-variance production they are neglected in single-mode theory. Our multi-mode numerical experiments have shown that the toroidal velocity is much smaller than the poloidal velocity except for large-wavenumber modes in large-Rayleigh-number convection (see Marcus 1980*b*).

Unlike expansions with more than one horizontal mode, the single-mode solutions are always time independent. Toomre *et al.* (1977), working with a plane-parallel geometry, also found that a single mode always leads to a steady-state solution. Expansions with a single mode suffer not only from the effects of truncation mentioned in the previous section, but also from other problems. For example, the correlation between the radial velocity and temperature,

$$\delta \equiv \langle \tilde{T}V_r\rangle / \langle \tilde{T}^2\rangle^{\frac{1}{2}} \langle V_r^2\rangle^{\frac{1}{2}}, \tag{2.33}$$

is always identically equal to 1 for a single mode; whereas, experimentally, Deardorff & Willis (1967) have found that the correlation in air for Rayleigh–Bénard convection is between 0·5 and 0·7 for Rayleigh numbers between 6×10^5 and 10^7. Far from the boundary the convective flux, $\langle TV_r\rangle$, that is predicted by single-mode theory is in good agreement with the flux predicted from multi-mode calculations (see § 3). Because the single mode overestimates δ, it always underestimates $\langle \tilde{T}^2\rangle \langle V_r^2\rangle$, the product of the thermal variance and radial component of the kinetic energy. Another peculiarity of the single-mode equations is that the thickness of the boundary layer at the surface is controlled by viscosity and decreases as the Rayleigh number is increased (see Toomre *et al.* 1977). In a real fluid we would expect the boundary layer to become turbulent and wide as the radially moving fluid smashes into the impermeable outer boundary. The thickness of the turbulent boundary layer is not regulated by viscosity, but by the rate at which energy can be transferred to other modes. The increase in boundary-layer thickness due to the nonlinear cascade in a multi-mode calculation has been reported by this author elsewhere (Marcus 1980*a*). In a single-mode calculation with a large Rayleigh number and an artificially thin boundary layer, most of the dissipation of kinetic energy takes place near the surface with

$$\langle\langle E_{\text{out}}\rangle\rangle \approx 4\pi\sigma \int_{1-\chi}^{1} (\mathbf{v}\cdot\nabla^2\mathbf{v})\,r^2\,dr, \tag{2.34}$$

where χ is the thickness of the boundary layer. From equation (2.34) we see that $\langle\langle E_{\text{out}}\rangle\rangle$ is proportional to $1/\chi$. Therefore, a single-mode calculation can compensate for its loss of dissipation in the missing high-wavenumber modes by decreasing χ.

(*f*) *Lorenz model*

A further truncation of single-mode expansion gives us the Lorenz model. Using the equilibrium conductive temperature gradient with the single-mode equations, we can compute the complete set of orthonormal eigenmodes of the velocity and temperature (as functions of radius). By expanding the radial dependence of the velocity and temperature in terms of these eigenmodes, substituting the expansions into the single-mode equations and retaining only a single mode in the radial expansion, we obtain the Lorenz equations. These equations were originally derived for a convecting fluid in a plane-parallel geometry, but they can easily be extended to a spherical geometry. The Lorenz model not only suffers from all of the physical approximations of the single-mode theory but also contains some additional limitations. Because the functional form of the velocity and fluctuating temperature are fixed and only their amplitudes are allowed to vary, the fluid can never develop boundary layers to help dissipate the kinetic and thermal energy. More importantly, because the functional forms of the velocity and temperature are fixed, the mean-temperature gradient cannot become isothermal.

If we were interested in computing solutions only when the Rayleigh number is slightly greater than its critical value, it would be practical to expand the velocity and temperature in the eigenmodes that are calculated with the conductive temperature gradient. However, these are not a very useful set of functions in which to expand the velocity and temperature when the Rayleigh number is large. For example, for any large Rayleigh number, we can choose a complete basis in which to expand the velocity and temperature by calculating the fundamental and all of the higher harmonic solutions to the single-mode equations. By retaining only the fundamental mode in the expansion, a modified set of Lorenz-type equations is obtained. We have computed the steady-state solutions to the regular spherical Lorenz equation and to the new modified Lorenz equations for a Rayleigh number ~ 30 times greater than the critical value for the onset of convection. The solution to the regular Lorenz equation is unstable with respect to time-dependent perturbations; both the solution to the modified Lorenz equation and the steady-state solution to the multi-mode equations with this Rayleigh number are stable. We conclude that qualitative description of the Lorenz model is not accurate for large Rayleigh numbers.

3. Numerical results of multi-mode calculations

In this section we present the numerical results of multi-mode calculations for $\sigma = 10$ and Rayleigh numbers of 10^4 and 10^5. For each Rayleigh number we repeat the calculation several times, each time using a different set of modes to show the effects of truncation. For all calculations, the heat source $H(r)$ (see equation (2.13)) is constant for $r \leqslant 0{\cdot}3$ and zero elsewhere.

(*a*) $Rs = 10^4$

To compute solutions to the modal equations, we have chosen the set of modes in the Galerkin expansion to be all of the spherical harmonics, $Y^{l,m}$ with $l \leqslant l_{\text{cutoff}}$, and all m. The radial dependence is finite-differenced with 128 grid points. For $l_{\text{cutoff}} = 3, 6, 9$ and 12 we find that the solution is time independent. A complete description of the

l_{cutoff}	$\langle T(0)\rangle$	E_{in}	Q_{in}
12	0·686	$4{\cdot}94\times10^{5}$	4·08
9	0·685	$4{\cdot}94\times10^{5}$	4·01
6	0·675	$4{\cdot}90\times10^{6}$	3·93
3	0·528	$4{\cdot}44\times10^{5}$	1·71

TABLE 1

solution with $l_{\text{cutoff}} = 12$ appears elsewhere (Marcus 1980*a*). To compare the overall features of the truncated solutions, we have listed the central temperature, E_{in} and Q_{in} as a function of l_{cutoff} in table 1. There is virtually no difference in the calculated values of $\langle T(0)\rangle$, E_{in} or Q_{in} for $l_{\text{cutoff}} = 6$, 9, and 12, which indicates that modes with $l > 6$ are not important in production, transport or dissipation of energy. Using the value of E_{in} from table 1, we find that the Kolmogorov length is $\sim 0{\cdot}212$ which approximately corresponds to a wavenumber $l \sim 4$. The solution with $l_{\text{cutoff}} = 3$ shows the effects of truncation; the rate of input of thermal energy for $l_{\text{cutoff}} = 3$ is nearly 60% lower than it is for $l_{\text{cutoff}} = 12$. The rate E_{in} for $l_{\text{cutoff}} = 3$ is nearly equal to E_{in} for $l_{\text{cutoff}} = 12$. The large decrease in Q_{in} is consistent with the analysis presented in § 2 which shows that the fluid can compensate for the loss of the thermally diffusive modes by decreasing Q_{in}. E_{in} is constrained by the fact that it must always be approximately equal to

$$4\pi\sigma Rs\int_0^1 \mathscr{L}(r)\,r\,dr = 4{\cdot}94\times10^{5}.$$

To compensate for the loss of the high wavenumber modes that dissipate the thermal variance when $l_{\text{cutoff}} = 3$, the fluid decreases Q_{in} by making the temperature gradient more nearly isothermal. The isothermal nature of the $l_{\text{cutoff}} = 3$ solution can be seen by noting that the central temperature for $l_{\text{cutoff}} = 3$ is less than it is for $l_{\text{cutoff}} = 12$.

A more sensitive probe of the effects of truncation is the kinetic and thermal energy spectra as functions of the horizontal wavenumber. In table 2 we have listed $Q(l, r = 0{\cdot}5)$, which is the two-dimensional thermal variance spectrum at $r = 0{\cdot}5$, with wavenumber l, i.e.

$$Q(l,r) = 2\pi\sum_{\gamma,m}(T_{\gamma,l,m})^2 r^2. \tag{3.1}$$

We have also listed the kinetic energy spectra, $E(l, 0{\cdot}5)$, at $r = 0{\cdot}5$, as functions of l and l_{cutoff} in table 3. The kinetic energy spectra show that the value of $E(l_{\text{cutoff}}, r = 0{\cdot}5)$ is higher than it should be. As pointed out in § 3, the truncation causes an upward curl in the energy spectrum at l_{cutoff} because the energy that cascades down from the large-scale modes piles up at l_{cutoff}. The upward curl at the large-wavenumber end of the spectrum is even more pronounced in the thermal variance spectra. Because the Prandtl number is greater than unity, the dissipation of thermal energy is less efficient than the diffusion of kinetic energy. The thermal variance does not dissipate in the production modes as does the kinetic energy and is free to cascade down the spectrum and pile up at the large wavenumbers. For the severest truncation, $l_{\text{cutoff}} = 3$, the thermal energy spectrum has inverted itself and $Q(3, 0{\cdot}5) > Q(2, 0{\cdot}5) > Q(1, 0{\cdot}5)$.

	l_{cutoff}			
l	12	9	6	3
1	$1{\cdot}37\times10^{-3}$	$1{\cdot}30\times10^{-3}$	$1{\cdot}19\times10^{-3}$	$3{\cdot}05\times10^{-3}$
2	$7{\cdot}89\times10^{-3}$	$7{\cdot}81\times10^{-3}$	$7{\cdot}66\times10^{-3}$	$1{\cdot}02\times10^{-2}$
3	$7{\cdot}19\times10^{-3}$	$7{\cdot}00\times10^{-3}$	$6{\cdot}85\times10^{-3}$	$3{\cdot}55\times10^{-2}$
4	$3{\cdot}95\times10^{-3}$	$4{\cdot}01\times10^{-3}$	$3{\cdot}81\times10^{-3}$	—
5	$1{\cdot}43\times10^{-4}$	$1{\cdot}44\times10^{-3}$	$1{\cdot}25\times10^{-3}$	—
6	$9{\cdot}62\times10^{-4}$	$9{\cdot}65\times10^{-4}$	$1{\cdot}81\times10^{-3}$	—
7	$2{\cdot}81\times10^{-4}$	$2{\cdot}91\times10^{-4}$	—	—
8	$1{\cdot}25\times10^{-4}$	$1{\cdot}30\times10^{-4}$	—	—
9	$2{\cdot}86\times10^{-5}$	$3{\cdot}01\times10^{-5}$	—	—
10	$1{\cdot}25\times10^{-5}$	—	—	—
11	$2{\cdot}35\times10^{-6}$	—	—	—
12	$2{\cdot}80\times10^{-6}$	—	—	—

TABLE 2. $Q(l, r=0{\cdot}5)$.

	l_{cutoff}			
l	12	9	6	3
1	1181	1182	1179	1174
2	535	534	532	628
3	213	211	207	273
4	32·7	31·6	30·8	—
5	7·03	6·89	6·92	—
6	2·92	2·87	2·99	—
7	0·579	0·578	—	—
8	0·204	0·205	—	—
9	$3{\cdot}75\times10^{-2}$	$3{\cdot}86\times10^{-2}$	—	—
10	$1{\cdot}48\times10^{-2}$	—	—	—
11	$3{\cdot}00\times10^{-3}$	—	—	—
12	$1{\cdot}99\times10^{-3}$	—	—	—

TABLE 3. $E(l, 0{\cdot}5)$.

(*b*) $Rs = 10^5$

For a Rayleigh number of 10^5 and a Prandtl number of 10, we have computed solutions for $l_{cutoff} = 12, 9, 6, 4, 3, 2$ and 1. With $l_{cutoff} = 1$ the solution is steady-state and the multi-mode equations reduce to those of single-mode theory. For a comparison between single and multi-mode solutions, we have plotted the kinetic energy of the $l = 1$ mode as a function of radius in figure 1 (solid line). Superimposed on this figure is the kinetic energy of the $l = 1$ mode (broken line) computed from the steady-state solution of the multi-mode equation with $l_{cutoff} = 12$. The functional form of the two curves is quite similar, the main difference being that the single-mode kinetic energy is consistently higher than the multi-mode solution. This difference in height confirms the predictions we made in § 2: the kinetic energy of the single mode must be enhanced to increase its rate of viscous dissipation. For the single mode, E_{out} is $4{\cdot}24\times10^6$, whereas for the $l = 1$ component of the multi-mode solution, E_{out} is only $3{\cdot}13\times10^6$. Approximately 32 % of the kinetic energy produced in the $l = 1$ component of the multi-mode solution is lost not through dissipation but through the nonlinear energy cascade.

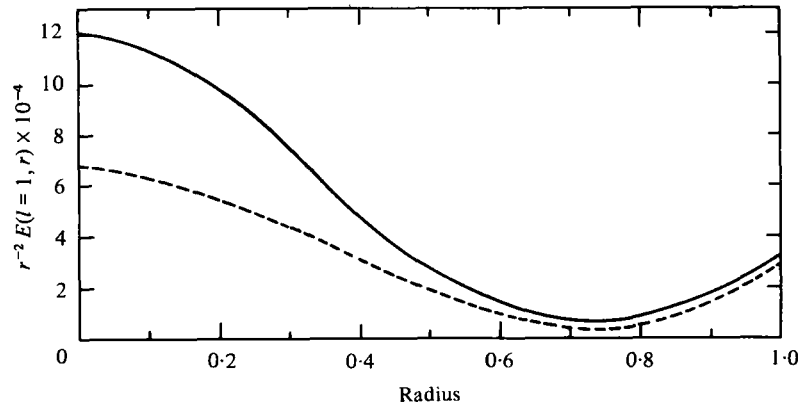

FIGURE 1. The kinetic energy for the $l = 1$ mode as a function of radius calculated with $l_{\text{cutoff}} = 1$ (solid line) and $l_{\text{cutoff}} = 12$ (broken line). The higher kinetic energy in the single-mode calculation allows more kinetic energy to be viscously dissipated and compensates for the inability of the single-mode calculation to lose energy by cascading. $Rs = 10^5$.

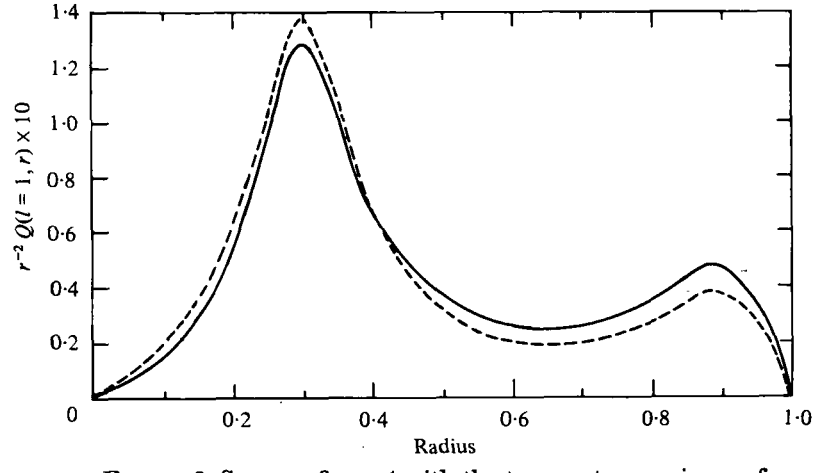

FIGURE 2. Same as figure 1 with the temperature variance of the $l = 1$ mode plotted as a function of radius.

In figure 2 we have plotted the temperature variance of the $l = 1$ mode of the multi-mode solution (broken line) and the single-mode solution (solid line). As in figure 1, the two curves have the same function form, but, in general, the single-mode thermal variance is greater than the multi-mode variance. The greater thermal variance allows the single mode to increase its rate of thermal dissipation. The rates at which the temperature variance is dissipated from the $l = 1$ components of the single- and multi-mode solutions are 0·293 and 0·231 respectively.

For all solutions computed with $l_{\text{cutoff}} \geqslant 4$, the solutions are steady-state and show truncation effects similar to those found for $Rs = 10^4$. For $l_{\text{cutoff}} = 4$, the temperature spectrum is inverted with $Q(l+1, 0{\cdot}5) > Q(l, 0{\cdot}5)$. The kinetic energy spectrum is not inverted. In figure 3 we have plotted $C \equiv E(l=2,\ r=0{\cdot}5)/E(l=3,\ r=0{\cdot}3)$ as a function of l_{cutoff}. C is a measure of the upward curl of the kinetic energy spectrum at

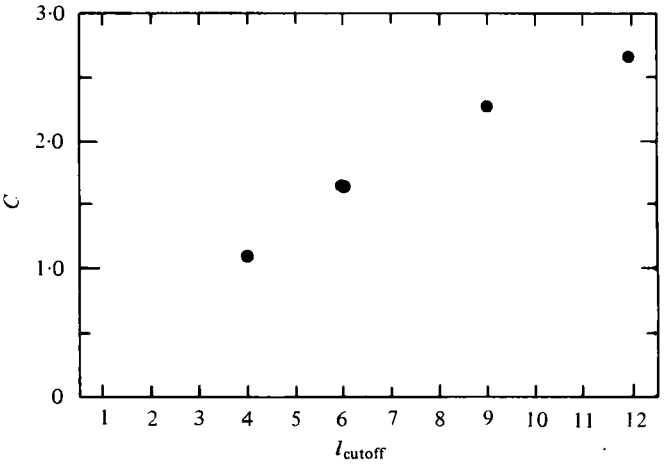

FIGURE 3. $C = E(l = 2,\ r = 0{\cdot}5)/E(l = 3,\ r = 0{\cdot}5)$ as a function of l_{cutoff}. Truncation causes the high-wavenumber modes of the kinetic energy spectrum to become anomalously large. By extrapolation, it appears that, when $l_{\text{cutoff}} = 3$, $C < 1$, meaning that the kinetic energy spectrum has become inverted.

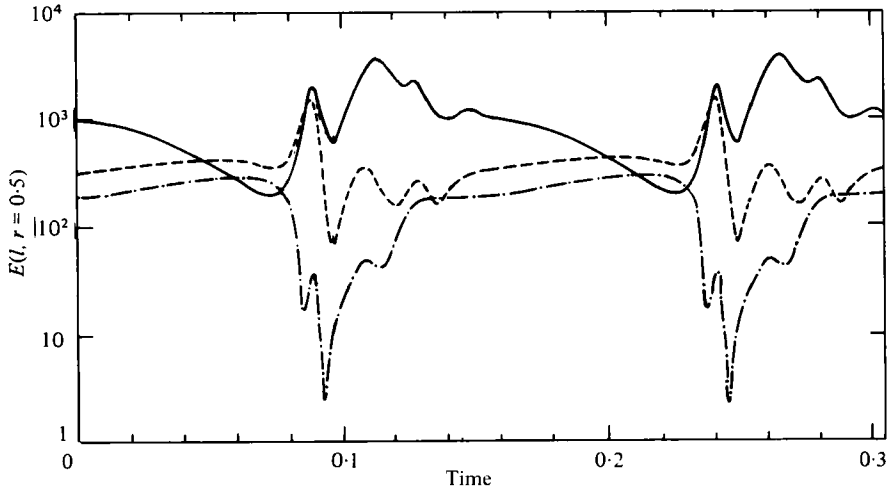

FIGURE 4. The kinetic energy calculated with $l_{\text{cutoff}} = 3$ at $r = 0{\cdot}5$ for the $l = 1$, 2 and 3 modes as a periodic function of time. At $t = 0{\cdot}0603$ kinetic energy inverts so that

$$E(l = 1,\ r\ 0{\cdot}5) < E(l = 3,\ r = 0{\cdot}5).$$

——, $l = 1$; – – –, $l = 2$; —·—, $l = 3$.

$l = 3$. If there were no truncation effects, we would expect C always to be greater than 1. If C becomes less than 1, it means that the kinetic energy spectrum is inverted, i.e. $E(l = 3,\ r = 0{\cdot}5) > E(l = 2,\ r = 0{\cdot}5)$. Figure 3 shows that C is greater than 1 but decreases as l_{cutoff} decreases. By extrapolating the points in figure 3, we may expect that C is less than 1 for $l_{\text{cutoff}} = 3$. For $l_{\text{cutoff}} = 3$ the solution is no longer steady-state but is periodic in time. The kinetic energy calculated with $l_{\text{cutoff}} = 3$ at $r = 0{\cdot}5$ as a function of wavelength, l, and as a function of time is plotted in figure 4 for one period of the fluid's oscillation.

We have arbitrarily labelled the left-hand axis of figure 4 as $t = 0$ but, in fact, it takes many iterations for the transients in the fluid to settle down and for the motions to become periodic. At $t = 0$, the kinetic energies of the $l = 1$, 2 and 3 wavelengths are similar in value to the stationary values obtained with $l_{\text{cutoff}} = 12$. As time increases, the kinetic energy of $l = 2$ and $l = 3$ modes increases; they are unable to dissipate their kinetic energy as fast as it cascades into (or is produced in) the modes. At $t = 0{\cdot}0467$ the kinetic energy of the $l = 1$ mode becomes less than that of the $l = 2$ mode, and at $t = 0{\cdot}0603$ the kinetic energy of the $l = 1$ and $l = 3$ modes cross. At this point in time, the kinetic energy spectrum changes quickly and re-establishes the $l = 1$ mode as the one with the largest amount of kinetic energy. By $t = 0{\cdot}152$, the solution settles down from its rapid oscillations. The period of the energy spectrum is $t_p = 0{\cdot}1528$; however, the period of temperature and velocity is $2t_p$. We have found that $\tilde{T}(t+t_p) = -\tilde{T}(t)$ and $\mathbf{v}(t+t_p) = -\mathbf{v}(t+t_p)$. If we assume that the characteristic velocity of the fluid is $[2E(l = 1, r = 0{\cdot}5)|_{t=0}]^{\frac{1}{2}}$, then we can estimate the eddy turnover time, t_e, to be $[2E(l = 1, r = 0{\cdot}5)|_{t=0}]^{-\frac{1}{2}}$ or $0{\cdot}022$. The period of the spectrum, t_p, is $6{\cdot}95t_e$. We have repeated the calculation with $l_{\text{cutoff}} = 3$ and with the viscosity of the $l = 3$ mode (but not the $l = 1$ or 2 modes) increased by 10 %. With the enhanced viscosity the solution is steady-state. When we increased the thermal diffusivity of the $l = 3$ mode by 10 %, the solution remained periodic in time. When $l_{\text{cutoff}} = 2$, the solution is aperiodic in time. The time-dependent behaviour is somewhat reminiscent of the strange attractor solution of the Lorenz model in the following sense. The kinetic energies of the $l = 1$ and $l = 2$ modes vary nearly periodically in time with $E(l = 1) \approx 10^3$ and $E(l = 2) \approx 10$. The small amplitudes of the nearly periodic oscillation slowly increase until a time when the flow quickly changes character and the kinetic energy spectrum becomes inverted with $E(l = 1) \approx 10^4$ and $E(l = 2) \approx 10^2$. The energies again vary almost periodically, with their oscillations growing in amplitude until the flow suddenly changes back to the original flow with $E(l = 1) \approx 10^3$ and $E(l = 2) \approx 10$. We have followed several of these changes from the $E(l = 1) \approx 10^4$ state to the $E(l = 1) \approx 10$ state and the flow never exactly repeats itself. We have not attempted to determine the fixed points of the flow nor have we calculated a Landau expansion to determine whether there might be an inverted bifurcation as there is with the Lorenz model.

4. Discussion

It is tempting to model the equations of motion by using a Galerkin truncation and retaining only the gravest modes to describe convection. It is likely that a truncation is justified if the dissipative modes as well as those modes responsible for energy production and transport are included. An easy way, of course, to show that all of the physically important wavelengths are resolved is to repeat the calculation with an increased number of modes and have the solutions remain unchanged. We have predicted and numerically confirmed (for a Rayleigh number of 10^4 and a Prandtl number of 10) that a truncation with an insufficient number of horizontal modes will accurately predict the rate of energy production but will: (1) alter the kinetic and thermal spectra by increasing the amplitudes of the high-wavenumber modes; (2) make the mean temperature gradient more isothermal and thereby lower the central temperature; and (3) decrease the rate at which the temperature variance is produced in the fluid. We have further shown that, if the truncation is too severe, the thermal

variance spectrum will become inverted, with the high-wavenumber dissipation modes having more energy than the low-wavenumber production modes. For $Rs = 10^4$, $\sigma = 10$ the thermal variance inversion does not destroy the time-independent property of the fluid. We have also predicted and numerically confirmed that single-mode calculation produces artificially thin boundary layers (where the thickness is determined by the actual viscosity and not the eddy viscosity). These thin boundary layers are needed to dissipate the kinetic energy that is generated from the buoyancy. If the dissipative modes had been included in the calculation, the kinetic energy would have been lost primarily through a turbulent cascade and not in a viscous boundary layer.

Modal representation can be used to predict transitions to time dependence in convective flow if sufficient care is taken so that enough modes are included to resolve all of the important length scales. Clever & Busse (1974) computed the bifurcation from steady-state rolls to time-dependent wavy rolls and have shown that their truncation is valid because the amplitudes of the velocity and temperature fluctuations are small. On the contrary, the transitions to aperiodicity reported by Curry (1978) and McLaughlin & Martin (1975) occur at large amplitudes and the Kolmogorov lengths are smaller than the limits of resolutions of their truncations. Their sequences of transitions would be more credible if more modes had been included. Even with 168 modes in spherical convection we find that when the flow changes to aperiodic the dissipative lengths are no longer resolvable and we cannot be certain that the transition is correct. Gollub & Benson (1980) have measured that the bifurcation to aperiodicity in plane-parallel convection with a Prandtl number of 2·5 occurs at a velocity of $\sim 0{\cdot}04\,\mathrm{cm\,s^{-1}}$. Since the thermal diffusivity is $\sim 1{\cdot}5 \times 10^{-3}$ and the horizontal dimensions of their cells are $\sim 3 \times 1{\cdot}5\,\mathrm{cm}$, the thermal dissipation length is $\sim 0{\cdot}1\,\mathrm{cm}$. This means that we would require 25×12 horizontal modes to resolve the dissipative length scales. An optimist might argue that although the model calculations do not include the dissipative length scales they may still be qualitatively correct despite the fact that the bifurcations are not at the exactly predicted Rayleigh number. The pessimist might argue that, if a theorist were provided with an experimentally determined sequence of bifurcations, he could probably find a set of nonlinear autonomous equations that qualitatively reproduced the sequence and then find a set of modes that correspond to his set of nonlinear equations. Our final caution is illustrated by considering the single-mode equations, which are a function of time and one spatial dimension. Although the single-mode equations do not correspond to any physical system they are nonlinear and share many of the properties of actual nonlinear equations that govern convection. From our numerical experiments and those of Toomre *et al.* (1977) it appears that the single-mode equations always admit at least one stable, steady-state solution for all Rayleigh numbers. If we examine the transition to time dependence of these equations using a Galerkin expansion in the vertical co-ordinate we would arrive at some erroneous conclusions. With one vertical mode we obtain the Lorenz model that predicts a bifurcation to a strange attractor, which is incorrect. An important feature of the single-mode solution is the development of thin boundary layers which provide a place for the kinetic energy to dissipate and whose thickness decreases with Rayleigh number. As the Lorenz model is supplemented with an increasing number of Fourier modes there will always be some Rayleigh number for which the Galerkin truncation can no longer resolve the boundary layers.

We conjecture that any Galerkin truncation of the single-mode equation always produces an erroneous bifurcation to time dependence at the Rayleigh number at which the boundary layers become unresolvable.

I thank the National Center for Atmospheric Research for use of their computing facility and D. Stewart for help in preparing the manuscript. This work was supported in part by National Science Foundation Grants ATM 76-10424 and AST 78-20708 and NASA Grant NGR-33-010-186.

REFERENCES

CHANDRASEKHAR, S. 1961 *Hydrodynamic and Hydromagnetic Stability.* Oxford University Press.

CLEVER, R. M. & BUSSE, F. H. 1974 Transition to time-dependent convection. *J. Fluid Mech.* **66**, 67–79.

CURRY, J. H. 1978 A generalized Lorenz system. *Commun. Math. Phys.* **60**, 193–204.

DEARDORFF, J. W. & WILLIS, G. E. 1967 Investigation of turbulent thermal convection between horizontal plates. *J. Fluid Mech.* **28**, 657–704.

GOLLUB, J. P. & BENSON, S. V. 1980 Time-dependent instabilities and the transition to turbulent convection. *J. Fluid Mech.* **100**, 449–470.

LATOUR, J., SPIEGEL, E. A., TOOMRE, J. & ZAHN, J.-P. 1976 Stellar convection theory. I. The anelastic modal equations. *Astrophys. J.* **207**, 233–243.

LORENZ, E. N. 1963 Deterministic nonperiodic flow. *J. Atmos. Sci.* **20**, 130–141.

MCLAUGHLIN, J. B. & MARTIN, P. C. 1975 Transition to turbulence in a statically stressed fluid system. *Phys. Rev.* A **12**, 186–203.

MARCUS, P. S. 1978 Nonlinear thermal convection in Boussinesq fluids and ideal gases with plane-parallel and spherical geometries. Ph.D. thesis. Ann Arbor, MI: University Microfilms.

MARCUS, P. S. 1979 Stellar convection. I. Modal equations in spheres and spherical shells. *Astrophys. J.* **231**, 176–192.

MARCUS, P. S. 1980*a* Stellar convection. II. A multi-mode numeric solution for convection in spheres. *Astrophys. J.* **239**, 622–639.

MARCUS, P. S. 1980*b* Stellar convection. III. Convection at large Rayleigh numbers. *Astrophys. J.* **240**, 203–217.

RUELLE, D. & TAKENS, F. 1971 On the nature of turbulence. *Commun. Math. Phys.* **20**, 167–192.

TOOMRE, J., GOUGH, D. O. & SPIEGEL, E. A. 1977 Numerical solutions of single-mode convection equations. *J. Fluid Mech.* **79**, 1–31.

TOOMRE, J., ZAHN, J.-P., LATOUR, J. & SPIEGEL, E. A. 1976 Stellar convection theory. II. Single-mode study of the second convection zone in an A-type star. *Astrophys. J.* **207**, 545–563.